

RESEARCH ARTICLE

Open Access



microRNA-451a promoter methylation regulated by DNMT3B expedites bladder cancer development via the EPHA2/PI3K/AKT axis

Beibei Liu[†], Wei Sun[†], Wuyue Gao, Liqiang Li, Zhenxue Cao, Xiaohuai Yang, Jianmin Liu and Yuanyuan Guo^{*}

Abstract

Background: The downregulation of microRNA (miR)-451a has been reported in bladder cancer (BCa) tissues. Herein, we elucidated the role of miR-451a in BCa with the involvement of DNA methyltransferase 3B (DNMT3B).

Methods: We first screened the differentially expressed miRNAs from the serum of 12 BCa patients and 10 healthy controls in the BCa database GSE113486. Subsequently, we detected miR-451a expression and CpG island methylation of the promoter in BCa cells T24 and 5637 with DNMT3B knockdown. The downstream mRNAs of miR-451a were predicted by bioinformatics and KEGG enrichment analysis. Afterwards, the expression patterns of DNMT3B, miR-451a and erythropoietin-producing hepatocellular receptor tyrosine kinase class A2 (EPHA2) were altered in BCa cells to test the ability of cell proliferation, apoptosis, migration as well as invasion. Finally, the effect of miR-451a and DNMT3B was evaluated in vivo.

Results: miR-451a was significantly reduced in serum of BCa patients and cell lines. Moreover, the expression of DNMT3B in BCa cells was significantly increased, thus promoting methylation of the miR-451a promoter, resulting in miR-451a inhibition. Additionally, we found that miR-451a targeted and negatively regulated EPHA2, while EPHA2 could activate the PI3K/AKT signaling, driving BCa cell growth and metastasis.

Conclusions: Our study proposed and demonstrated that miR-451a downregulation mediated by DNMT3B is critical for proliferation, migration, and invasion of BCa, which may be beneficial for developing more effective therapies against BCa.

Keywords: Bladder cancer, DNMT3B, microRNA-451a, EPHA2, The PI3K/AKT signaling

Background

Bladder cancer (BCa), the most common and lethal cancer in the urinary system, holds accountable for estimated 81,400 new cases and 17,980 death in the USA in 2020 [1]. BCa is divided into two main categories, muscle-invasive BCa (accounting for 25%) and non-muscle invasive BCa

(accounting for 75%), and the former one is treated by radical cystectomy, adjuvant chemotherapy or chemoradiotherapy, while the latter one is usually treated by transurethral resection and intravesical therapies [2]. About half of non-muscle invasive BCa are low grade, whereas most muscle-invasive or metastatic BCa are high grade [3]. To significantly halt the course of the malignancy, improvements should be achieved in the diagnosis and treatment of metastatic BCa.

MicroRNAs (miRNAs) are endogenous ~23 nt RNA transcripts that play vital gene-regulatory roles in animals

* Correspondence: Guoyy04143@163.com

[†]Beibei Liu and Wei Sun contributed equally to this work.

Department of Urology, The First Affiliated Hospital of Bengbu Medical College, No. 287, Changhuai Road, Bengbu 233000, Anhui, People's Republic of China



© The Author(s). 2020 **Open Access** This article is licensed under a Creative Commons Attribution 4.0 International License, which permits use, sharing, adaptation, distribution and reproduction in any medium or format, as long as you give appropriate credit to the original author(s) and the source, provide a link to the Creative Commons licence, and indicate if changes were made. The images or other third party material in this article are included in the article's Creative Commons licence, unless indicated otherwise in a credit line to the material. If material is not included in the article's Creative Commons licence and your intended use is not permitted by statutory regulation or exceeds the permitted use, you will need to obtain permission directly from the copyright holder. To view a copy of this licence, visit <http://creativecommons.org/licenses/by/4.0/>. The Creative Commons Public Domain Dedication waiver (<http://creativecommons.org/publicdomain/zero/1.0/>) applies to the data made available in this article, unless otherwise stated in a credit line to the data.

and plants by matching mRNAs to direct their posttranscriptional repression [4]. Several miRNAs, including miR-205, miR-210, miR-124 and miR-214 have been elucidated as active players in BCa cell apoptosis, proliferation and differentiation [5]. Deep-sequencing-based BCa signatures conducted by Matsushita et al. suggested that clustered miRNAs, including miR-451a were downregulated in BCa tissues [6], with their specific role in BCa undetermined. Even though the mechanisms behind miRNA dysregulation in malignancies have not been clearly established, the silencing of several miRNAs has been suggested to correlated with epigenetic mechanisms, such as histone modification and DNA methylation [7]. For instance, it has been previously reported that upregulated heterochromatin protein 1 γ in prostate cancer cells repressed the expression pattern of miR-451a by promoting H3K9 methylation at the promoter region of miR-451a [8]. Therefore, we hypothesized that the declines in miR-451a expression in BCa was also in a correlation with methylation of its promoter region. Interestingly, methylation of cytosine and guanine (CpG) islands contributed to the knockdown of miR-502-5p in BCa, while DNA methyltransferase 3B (DNMT3B) and miR-502-5p established a feedback loop in the modulation of BCa [9]. Also, the level of DNMT3B was significantly promoted in BCa tissues and cells relative to the normal controls, and DNMT3B siRNAs reduced BCa cell proliferation, migration and invasion, whereas stimulated cell apoptosis [10]. Thus, we could reasonably postulate that miR-451a plays a tumor suppressor role in BCa in a DNMT3B-dependent manner. Therefore, this study was undertaken to probe whether miR-451a regulates BCa growth through DNMT3B-mediated methylation and the downstream biomolecules. This study may provide new and promising therapeutic targets for BCa treatment.

Methods

Cell lines, antibodies, vectors and reagents

5-aza-dC purchased from Sigma-Aldrich Chemical Company (St Louis, MO, USA) was dissolved in DMSO and configured into 5 μ M solution for further use. Urinary bladder transitional cell carcinoma cell T24 (#SCSP-536), urinary bladder grade II carcinoma cell 5637 (#TCHu 1), urinary bladder grade IV transitional cell carcinoma cell TCCSUP (#SCSP-571) and urinary bladder grade IV transitional cell carcinoma cell UM-UC3 (#SCSP-684, all BCa cell lines) were from Cell Bank of Shanghai Institute of Cells (Shanghai, China). Immortalized human uroepithelial cells SV-HUC-1 were from ATCC (Manassas, VA, USA, #CRL-9520). The antibodies used in the experiments were DNMT3B (#72335, Cell Signaling Technologies (CST), Beverly, MA, USA), phos-PI3K (#ab182651, Abcam, Cambridge, UK), phos-AKT1 (#44-621G, Thermo Fisher Scientific Inc.,

Waltham, MA, USA), EPHA2 (#37-4400, Thermo Fisher), KI67 (#9027, CST), glyceraldehyde-3-phosphate dehydrogenase (GAPDH, #ab181602, Abcam), horseradish peroxidase (HRP)-labeled goat anti-mouse (#G-21040, Thermo Fisher) or goat anti-rabbit IgG (#G-21234, Thermo Fisher). Terminal deoxynucleotidyl transferase (TdT)-mediated dUTPbiotin nick end labeling (TUNEL) kit was purchased from Promega (#G3250, Madison, WI, USA). 5-Ethynyl-2'-deoxyuridine (EdU) cell proliferation detection kit was obtained from Solarbio (#CA1170, Beijing, China). DMEM and FBS were from Gibco (Carlsbad, CA, USA). Short hairpin RNAs (shRNAs) targeting DNMT3B and corresponding Scramble shRNA (sh-NC), miR-451a inhibitor, inhibitor NC, miR-451a mimic, mimic NC (Mock), oe-NC and oe-EPHA2 were synthesized and purchased from OriGene Technologies (Beijing, China). Primer sequences used for quantitative reverse transcriptase-PCR (RT-qPCR) were synthesized by Shanghai Sangon Biological Engineering Technology & Services Co., Ltd. (Shanghai, China) and are presented in Table 1.

Bioinformatics analysis

First, we downloaded the BCa-related differentially expressed miRNA dataset GSE113486 from the GEO database (<https://www.ncbi.nlm.nih.gov/geo/>), and conducted the differential analysis with the R Limma package. A heatmap was plotted using the R pheatmap package with Log FoldChange > 2, p value < 0.05 as the threshold. We then analyzed DNMT3B expression in BCa patients and normal bladder tissues through the oncomine database (<https://www.oncomine.org/>) and the GEPIA database (<http://gepia.cancer-pku.cn/index.html>). The relationship between miR-451a expression and the survival of BCa patients was analyzed using KM-plotter website (<http://kmplot.com/analysis/>). Moreover, targeting mRNAs of miR-451a were predicted through StarBase website (<http://starbase.sysu.edu.cn/>). Then the online bioinformatics tool DAVID 6.8 (<https://david.ncifcrf.gov/>) was used to carry out KEGG analysis of the selected 448 mRNAs and to map the bubble chart using the ggplot2.

Cell culture and treatment

The T24 and 5637 cells were maintained in DMEM containing 10% FBS under 5% CO₂ at 37 °C. Cells were collected for subsequent assays when the cell confluence reached 75–85%. T24 and 5637 cells in good growth condition were transfected with DNMT3B shRNA, sh-NC, miR-451a inhibitor, inhibitor NC, miR-451a mimic, mimic NC (Mock), oe-NC and oe-EPHA2 vectors alone or in combination. Transfection was performed using Lipofectamine 2000 kits according to the instructions. The cells were harvested at 48 h post-transfection, and

Table 1 Primer sequences used in RT-qPCR

Targets	Forward (5'-3')	Reverse (5'-3')
miR-451a	ACACTCCAGCTGGGAAACCGTTACCATTAC	CTCAACTGGTGTCTGGAGTCGGCAATTCAGTTGAGCTTACAG
DNMT3B	TAACAACGGCAAAGACCGAGGG	TCCTGCCACAAGACAAACAGCC
EPHA2	ACTGCCAGTGTGACGATCAACC	GTGACCTCGTACTCCACACTC
U6	AAAGCAAATCATCGGACGACC	GTACAACACATTGTTTCCTC
GAPDH	CTGGGCTACACTGAGCACC	AAGTGGTCGTTGAGGGCAATG

Note: RT-qPCR quantitative reverse transcriptase-PCR, miR microRNA, DNMT3B DNA methyltransferase 3B, EPHA2 erythropoietin-producing hepatocellular receptor tyrosine kinase class A2, GAPDH glyceraldehyde-3-phosphate dehydrogenase

RT-qPCR was used to verify the transfection efficiency of the cells.

EdU assay

T24 and 5637 cells were seeded at 5000 cells/well in 96-well plates containing DMEM/F-12 medium and 50 mM EdU. After 12 h of culture, the cells were fixed with 4% paraformaldehyde, neutralized with 2 mg/mL glycine and infiltrated in 0.5% Triton X-100 for 10 min (all at room temperature). Apollo staining reaction buffer was then added for EdU immunostaining. The nuclei were labeled with Hoechst 33342, and EdU positive cells were counted from at least 500 cells under a fluorescence microscope (Olympus Ckx53, Olympus Optical Co., Ltd., Tokyo, Japan) and analyzed by Image J (National Institutes of Health, Bethesda, MD, USA).

Flow cytometry

T24 and 5637 cells under good growth condition were detached with 0.25% trypsin. Totally 10^6 cells were re-suspended with Annexin V binding buffer (BioLegend, San Diego, CA, USA) and added with 5 μ L APC Annexin V and 10 μ L propidium iodide (PI) solution. The cells were loaded onto a C6 instrument (BD Biosciences, San Jose, CA, USA) after an incubation at room temperature in void of light for 15 min.

TUNEL staining

The apoptosis was detected using TUNEL apoptosis detection kit (Promega) for T24 and 5637 cells. The cells were cultured with 20 μ g/mL protease K at room temperature for 20 min and incubated with fluorescein isothiocyanate-TUNEL buffer in the dark for 1 h. Phosphate buffered saline without TdT enzymes was set as a negative control. The nuclei were labeled with Hoechst 33342, and the images were obtained under a microscope. The percentage of TUNEL positive cells was counted from at least 500 cells.

Transwell assay

Cell invasion was detected using Transwell chambers (Corning Corporation, Midland, MI, USA). Briefly, the cells were placed into the apical chamber pre-coated

with Matrigel. The basolateral chamber was filled with DMEM. After 48 h of incubation, cells in the basolateral chamber were fixed in 4% paraformaldehyde for 15 min and stained with 0.1% crystal violet for 20 min. Finally, cells in five randomly selected fields were counted under an inverted microscope (200 \times , Ckx53, Olympus Optical Co., Ltd., Tokyo, Japan). For migration assay, the operation procedure was consistent with the invasion assay except for Matrigel coating.

RT-qPCR

Total RNA of tissues and cells was extracted with TRIzol (Sigma) reagent according to the protocols. miScript II RT kits (Takara Biotechnology Co., Ltd., Dalian, Liaoning, China) and SYBR Premix Ex TaqTM II (Takara) were used for reverse transcription and qPCR on an on-time ABI PRISM 7500 system.

Western blot

Radio immunoprecipitation assay protein extraction reagents (Beyotime, Shanghai, China) containing phenylmethanesulfonyl fluoride (Roche, Basel, Switzerland) were used for lysis. The protein samples were then separated using SDS-PAGE and transferred to polyvinylidene fluoride membranes (Millipore, Billerica, MA, USA). The membranes were then sealed with 5% non-fat milk for 2 h and probed for one night at 4 $^{\circ}$ C. Subsequently, the membranes were re-probed at 37 $^{\circ}$ C with HRP-labeled secondary antibody for a period of 1 h. Chemiluminescence was detected by the ECL substrate kit (Thermo Fisher Scientific Inc., Waltham, MA, USA) and subsequent exposure using ChemiDoc XRS imaging systems. Band density was analyzed using Image J software (National Institutes of Health, Bethesda, MD, USA) and normalized to GAPDH.

Promoter methylation detection

The genomic (g) DNA was isolated from T24 and 5637 cells with the help of the TIANamp gDNA kit (TIAN GEN Biotech Co., Ltd., Beijing, China). Subsequently, the gDNA was converted into DNA sodium hydrogen sulfite using the EpiTect Plus Bisulfite kit (Qiagen company, Hilden, Germany).

The methylation status of miR-451a was determined by methylation-specific PCR (MSP) using a Veriti96PCR thermal cycler (Applied Biosystems, Inc., Foster City, CA, USA) with Taq PCR MasterMix (TIANGEN Biotech Co., Ltd., Beijing, China). PCR products were run on 3% agarose gel and subsequently identified by ethidium bromide staining at room temperature. 160 bp products represent miR-451a methylation and 120 bp products represent miR-451a demethylation.

Chromatin immunoprecipitation (ChIP)

SimpleChIP Plus Sonication Chromatin IP (#56383S, Cell Signaling Technology, Danvers, MA, USA) was used for ChIP detection. About 1×10^7 cells were crosslinked in 1% formaldehyde for 10 min and quenched in glycine for 5 min at room temperature. The dissolved chromatin was incubated with Flag and IgG antibodies.

Luciferase activity assay

The wild-type (WT) EPHA2 promoter sequence containing binding sites with miR-451a was cloned into pmirGLO luciferase reporter vector (Promega), and mutant (MT) EPHA2 promoter sequence without binding sites was constructed into the same vector to generate report plasmids EPHA2-WT/EPHA2-MT. The 293 cells were co-transfected with 50 nM miR-451a mimic or NC mimic and 500 ng/mL reporter plasmids for 2 days. The luciferase intensity was assessed by a Dual-Glo[®] luciferase detection system (Promega).

Xenografts

Four-week-old NOD/SCID mice ($n = 20$) were purchased from Shanghai SLAC Laboratory Animal Co., Ltd. (Shanghai, China). Nude mice were arbitrarily categorized into four groups, with five mice in each group. All mice were allowed to acclimatize for 1 week in the animal facility before treatment. T24 cells (2×10^6) transfected with sh-NC, shDNMT3B, shDNMT3B + inhibitor NC or shDNMT3B + miR-451a inhibitor in 0.2 mL were injected subcutaneously in each flank of nude mice. Tumors were measured with a caliper at an interval of 5 days, and the tumor volume was calculated as $\pi \times \text{width}^2 \times \text{length} / 6$. The mice were euthanized by an intraperitoneal injection of excessive pentobarbital sodium after 35 days. At half an hour post-injection, the death of mice was confirmed by observing the lack of heartbeat, respiratory arrest, pupil dilation, and lack of nerve reflex. The tumor was subsequently collected for weight measurement and further examination. All animal experiments were compliant with ethic regulations and approved by Institutional Animal Care & Use Committee of the First Affiliated Hospital of Bengbu Medical College.

Immunohistochemistry

First, the paraffin-embedded sections fixed in formalin were dewaxed with xylene and incubated with 3% hydrogen peroxide to block endogenous peroxidase activity. After that, the sections were treated with 5% goat serum and incubated overnight with the primary antibody at 4 °C. The sections were then incubated with the biotinylated anti-mouse/rabbit IgG and with streptomycin-biotin peroxidase for 15 min. The immunostained images were captured from 10 different fields using a fluorescence microscope (Olympus Ckx53) at a 400 \times magnification and analyzed by Image J.

Statistical method

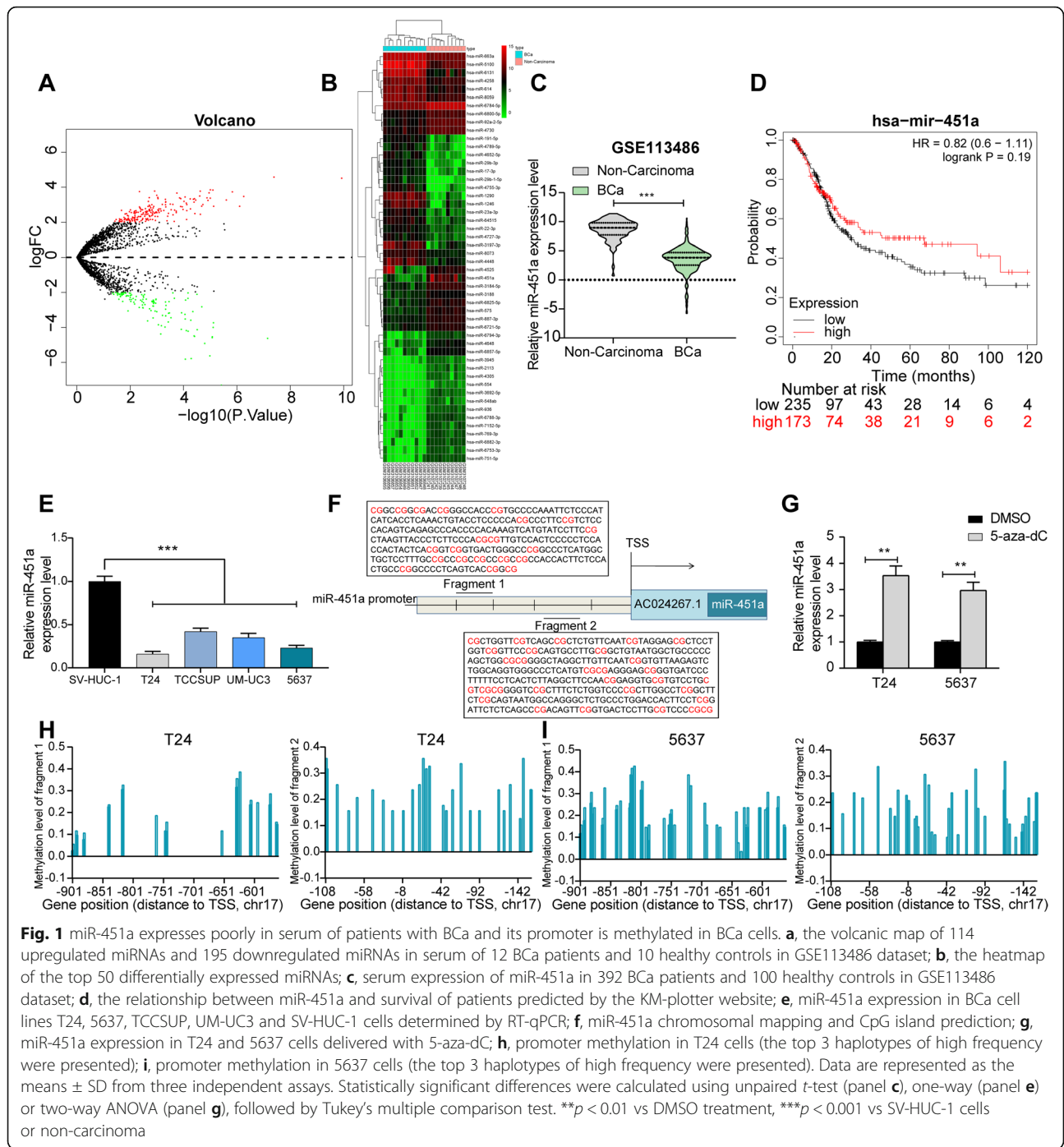
All experiments were repeated for at least three times. All data, presented by mean \pm standard deviation (SD), were analyzed using the statistical software SPSS 22.0 (IBM, Chicago, IL, USA) and Prism 8.0 (GraphPad, San Diego, CA, USA). Data among multiple groups were tested by one-way or two-way analysis of variance (ANOVA) with Tukey's post hoc test, and statistical significance was defined as a two-tailed value of $p < 0.05$.

Results

miR-451a is downregulated in serum of BCa patients and its promoter is methylated

Firstly, 309 differentially expressed miRNAs from the serum of 12 BCa patients and 10 healthy controls were screened out in GSE113486 by setting Log FoldChange > 2 , p value < 0.05 as the screening thresholds. Among them, 114 miRNAs were upregulated and 195 miRNAs were downregulated in BCa (Fig. 1a). The heatmap in Fig. 1b shows the top 50 differentially expressed miRNAs. Subsequently, we found that miR-451a was significantly reduced (Fig. 1c) in the serum of 392 BCa patients relative to that in 100 healthy control patients in the GSE113486 dataset. Moreover, the KM-plotter website revealed that BCa patients highly expressing miR-451a had longer survival time (Fig. 1d). We then examined the expression pattern of miR-451a in BCa cell lines T24, 5637, TCCSUP and UM-UC3 and immortalized human uroepithelial cells SV-HUC-1. The expression of miR-451a in BCa cell lines was significantly inhibited (Fig. 1e). These results suggest that miR-451a may play a potential regulatory role in BCa.

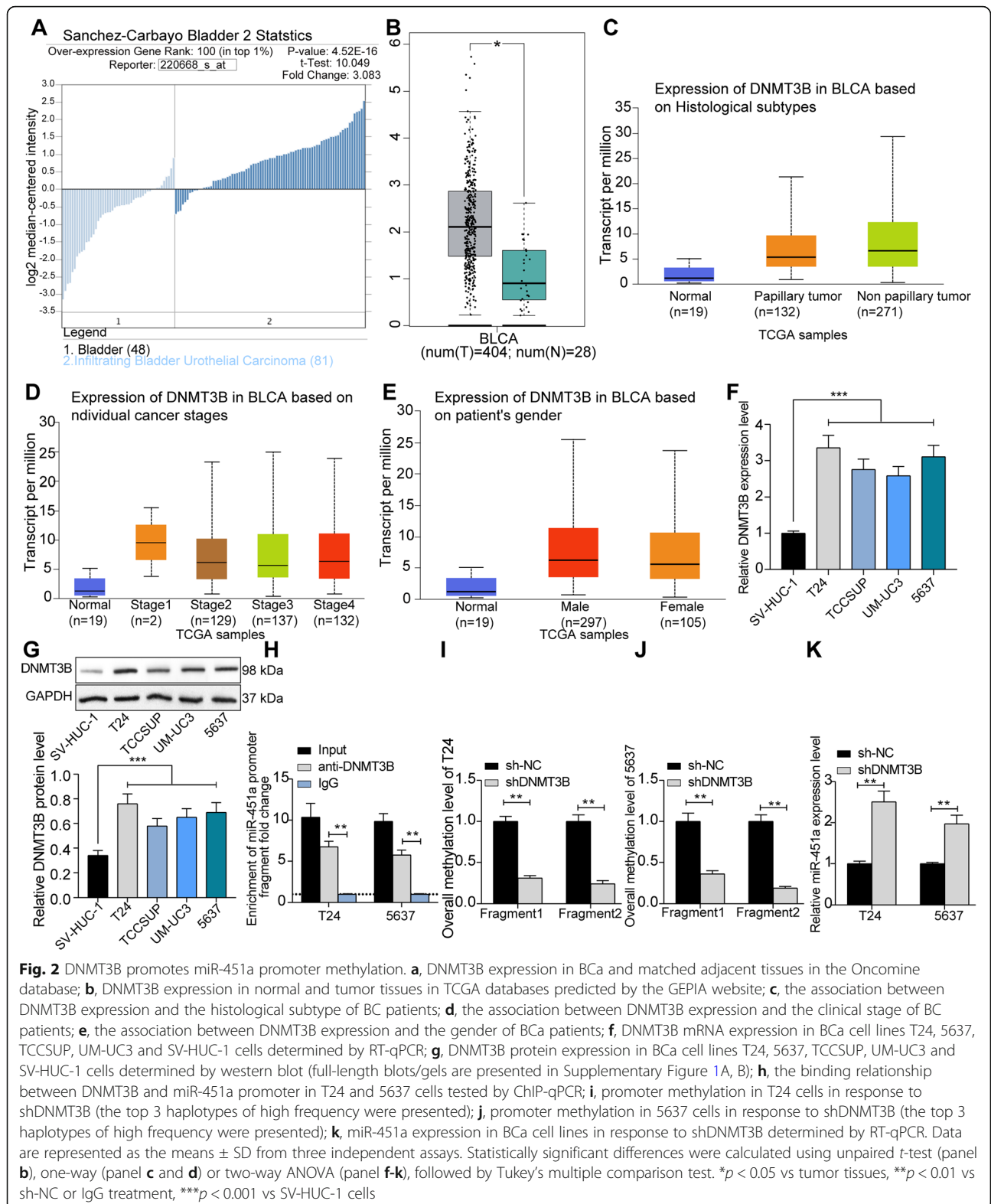
miR-451a is located on the chr17 chromosome and belongs to the AC024267.1 region (Fig. 1f). It has been previously displayed that miR-433 was frequently downregulated in BCa due to the methylation status of CpG islands in the promoter region [11]. To assess the AC024267.1 promoter methylation status and the regulatory role of miR-451a in BCa, miR-451a expression was increased in T24 and 5637 cell lines after 5'-aza-2'-deoxycytidine (5-aza-dC) treatment, as revealed by RT-



qPCR (Fig. 1g). Moreover, promoter methylation detection was performed to test the methylation level of miR-451a CpG island in T24 and 5637 cell lines. The results suggested that promoter methylation was responsible for miR-451a dysregulation in BCa (Fig. 1h, i). Therefore, the results indicated that miR-451a was downregulated in BCa due to hypermethylation of CpG islands, whereas miR-451a may play a tumor suppressor role in the BCa.

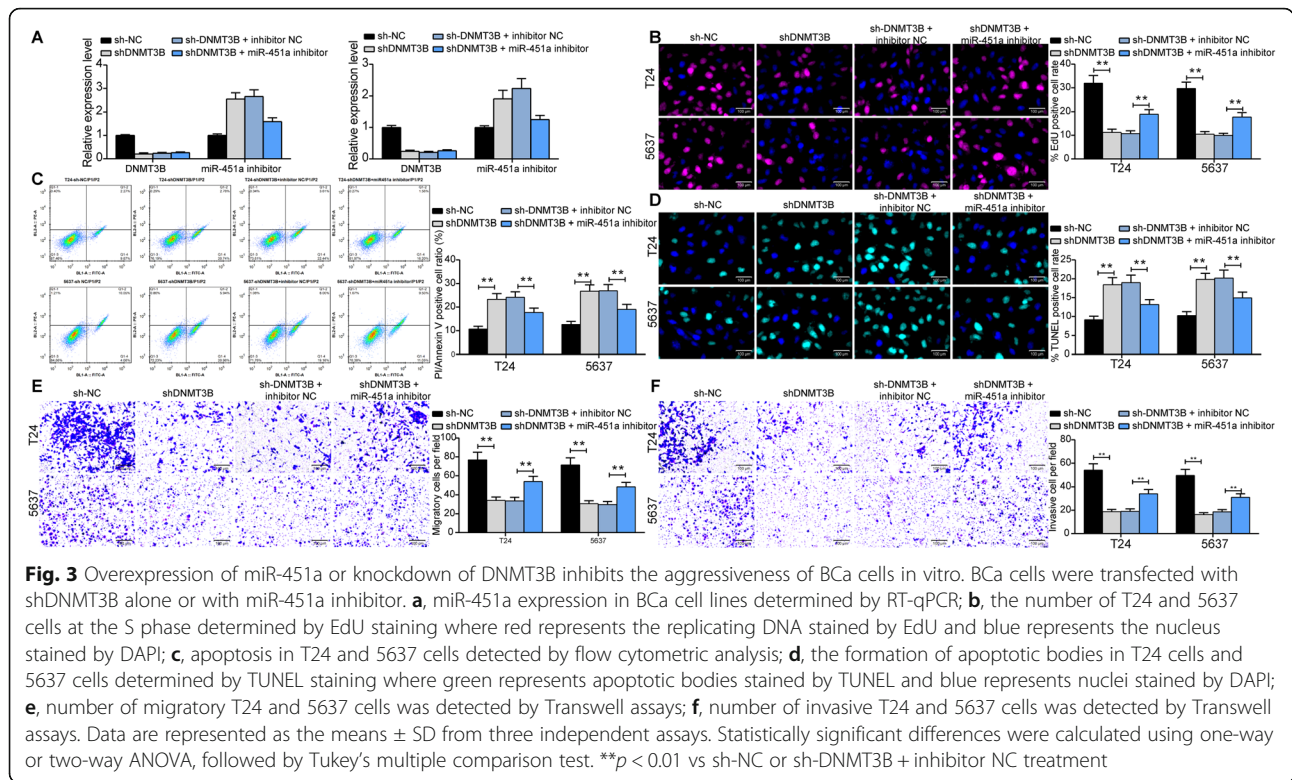
DNMT3B promotes miR-451a promoter methylation

To further investigate the upstream regulatory mechanism of miR-451a, we found through literature review that DNMTs could inhibit miR-200a expression by promoting methylation of the miR-200a promoter, thus promoting breast cancer cell growth [12]. Therefore, we first found that DNMT3B was significantly overexpressed (Fig. 2a) in the BCa through the OncoPrint database, and a same trend was observed in the bladder



urothelial carcinoma (BLCA) tissues using the GEPIA website (Fig. 2b). The association between the expression of DNMT3B and the clinical stage, histological

subtype, and gender of the patients in The Cancer Genome Atlas (TCGA) database was queried. We found no significant difference between the expression of



DNMT3B and the histological subtype (Fig. 2c), clinical stage (Fig. 2d) or gender (Fig. 2e) of BCa patients. Subsequently, a significant increase was observed in DNMT3B expression in BCa cell lines compared to SV-HUC-1 cells (Fig. 2f, g). Then, we used ChIP-qPCR experiments to find that fragments of miR-451a promoters in chromatin complexes precipitated using specific antibody against DNMT3B were significantly higher than IgG (Fig. 2h). Moreover, the methylation level of miR-451a promoters in T24 and 5637 cells was reduced (Fig. 2i, j) after DNMT3B knockdown, and miR-451a expression in cells was significantly increased (Fig. 2k).

Overexpression of miR-451a or knockdown of DNMT3B inhibits the aggressiveness of BCa cells in vitro

In order to assess the role of miR-451a and DNMT3B in the aggressiveness of BCa cells, we first knocked-down DNMT3B expression in T24 and 5637 cells. The results of the Fig. 2h demonstrated that miR-451a in these cells increased significantly after knocking down DNMT3B. Therefore, we further knocked-down miR-451a in cells, and RT-qPCR verified the successful transfection (Fig. 3a). The cell proliferation activity was repressed notably by shDNMT3B, which was restored by miR-451a inhibitor (Fig. 3b). Then, after PI/Annexin V staining and flow cytometry, the number of apoptotic T24 and 5637 cells was elevated significantly under the action of shDNMT3B, and further addition of miR-451a

inhibitor weakened the promoting role of shDNMT3B in the apoptosis of BCa cells (Fig. 3c). The TUNEL assay also exhibited the same experimental results (Fig. 3d). Then, we further used Transwell assays to detect the invasion and migration ability of cells. The number of cells that migrated or invaded to the basolateral chamber was significantly reduced after DNMT3B knockdown, but

Table 2 Enrichment analysis

Term	Count	p value
hsa04152AMPK signaling pathway	12	0
hsa04068FoxO signaling pathway	11	0.001
hsa04144Endocytosis	15	0.002
hsa04962Vasopressin-regulated water reabsorption	5	0.019
hsa04390Hippo signaling pathway	9	0.026
hsa04913Ovarian steroidogenesis	5	0.028
hsa00051Fructose and mannose metabolism	4	0.039
hsa04150mTOR signaling pathway	5	0.047
hsa04151PI3K-Akt signaling pathway	14	0.042
hsa05230Central carbon metabolism in cancer	5	0.041
hsa04022cGMP-PKG signaling pathway	8	0.009
hsa00100Steroid biosynthesis	3	0.014
hsa04622RIG-I-like receptor signaling pathway	5	0.002
hsa05205Proteoglycans in cancer	9	0.019

miR-451a inhibitor conferred migratory and invasive potentials to T24 and 5637 cells (Fig. 3e, f).

miR-451a impairs the PI3K/Akt signaling activity by targeting EPHA2

We focused our attention on miR-451a downstream regulatory mechanisms after studying the upstream regulatory mechanisms of miR-451a. The targeting mRNAs of miR-451a were firstly predicted by StarBase bioinformatics prediction website. A total of 458 mRNAs

were screened out. After that, we used DAVID bioinformatics online tool for enrichment analysis, and 14 signaling pathways were enriched (Table 2). The PI3K/AKT signaling was significantly enriched (Fig. 4a), and the activation the PI3K/AKT signaling was reported to significantly promote BCa cell proliferation and migration [13, 14]. Moreover, we found EPHA2 was in the upstream (Fig. 4b) of the PI3K/AKT signaling, and the tumor initiating role of EPHA2 has been indicated in BCa [15]. We subsequently examined the expression of

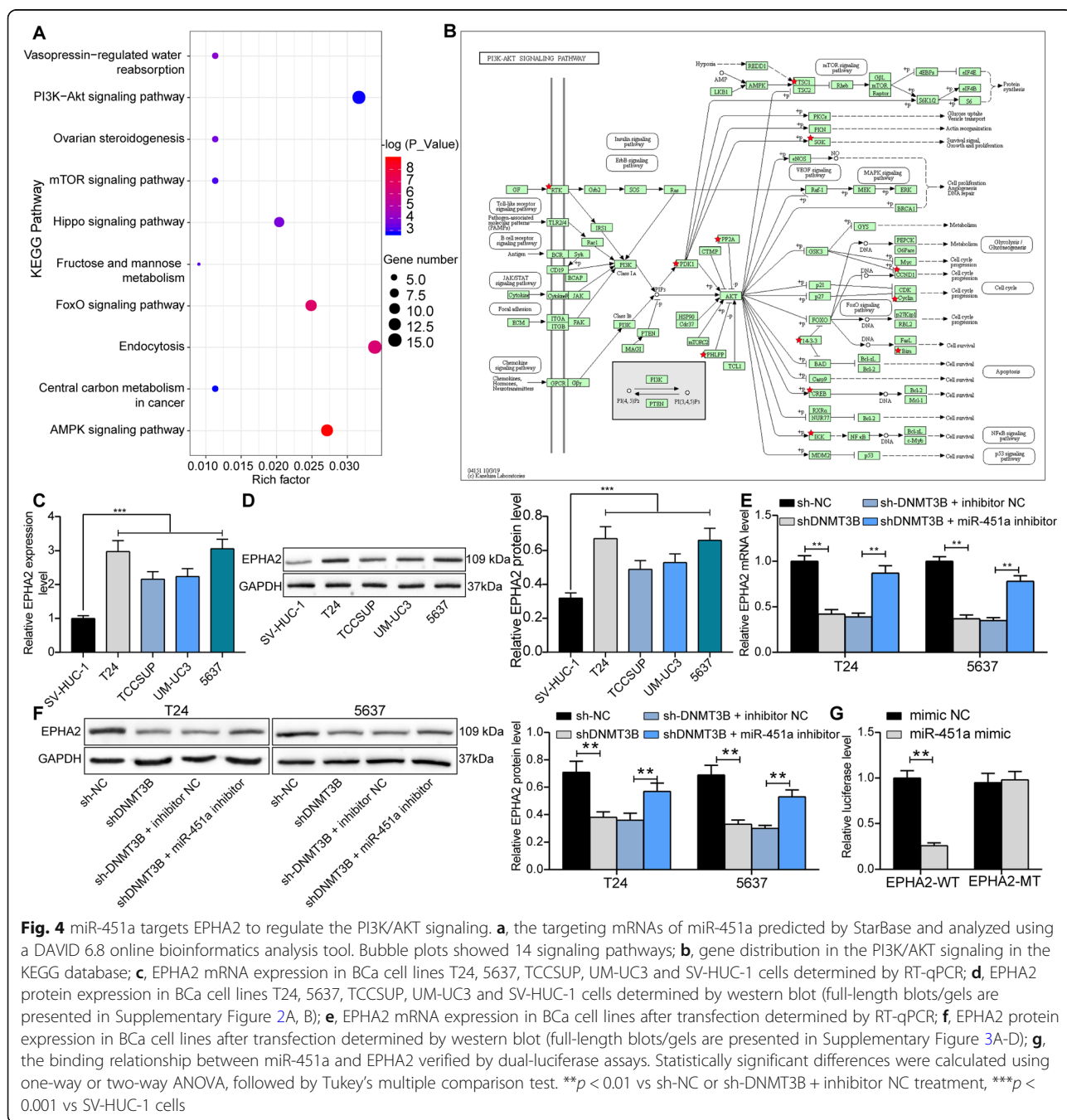


Fig. 4 miR-451a targets EPHA2 to regulate the PI3K/AKT signaling. **a**, the targeting mRNAs of miR-451a predicted by StarBase and analyzed using a DAVID 6.8 online bioinformatics analysis tool. Bubble plots showed 14 signaling pathways; **b**, gene distribution in the PI3K/AKT signaling in the KEGG database; **c**, EPHA2 mRNA expression in BCa cell lines T24, 5637, TCCSUP, UM-UC3 and SV-HUC-1 cells determined by RT-qPCR; **d**, EPHA2 protein expression in BCa cell lines T24, 5637, TCCSUP, UM-UC3 and SV-HUC-1 cells determined by western blot (full-length blots/gels are presented in Supplementary Figure 2A, B); **e**, EPHA2 mRNA expression in BCa cell lines after transfection determined by RT-qPCR; **f**, EPHA2 protein expression in BCa cell lines after transfection determined by western blot (full-length blots/gels are presented in Supplementary Figure 3A-D); **g**, the binding relationship between miR-451a and EPHA2 verified by dual-luciferase assays. Statistically significant differences were calculated using one-way or two-way ANOVA, followed by Tukey's multiple comparison test. ** $p < 0.01$ vs sh-NC or sh-DNMT3B + inhibitor NC treatment, *** $p < 0.001$ vs SV-HUC-1 cells

EPHA2 in T24, 5637, TCCSUP, UM-UC3 and SV-HUC-1 cells and noted that its expression in BCa cells were much higher than those in SV-HUC-1 cells (Fig. 4c, d). In addition, after DNMT3B knockdown, EPHA2 expression in T24 and 5637 cells was significantly inhibited, while EPHA2 expression was recovered (Fig. 4e, f) under the synergistic effect of shDNMT3B and miR-451a inhibitor. Consequently, we used dual-luciferase assays to test the binding relationship between miR-451a and EPHA2 3'UTR. The luciferase activity was significantly inhibited in 293 T cells delivered with miR-451a and EPHA2-WT (Fig. 4g).

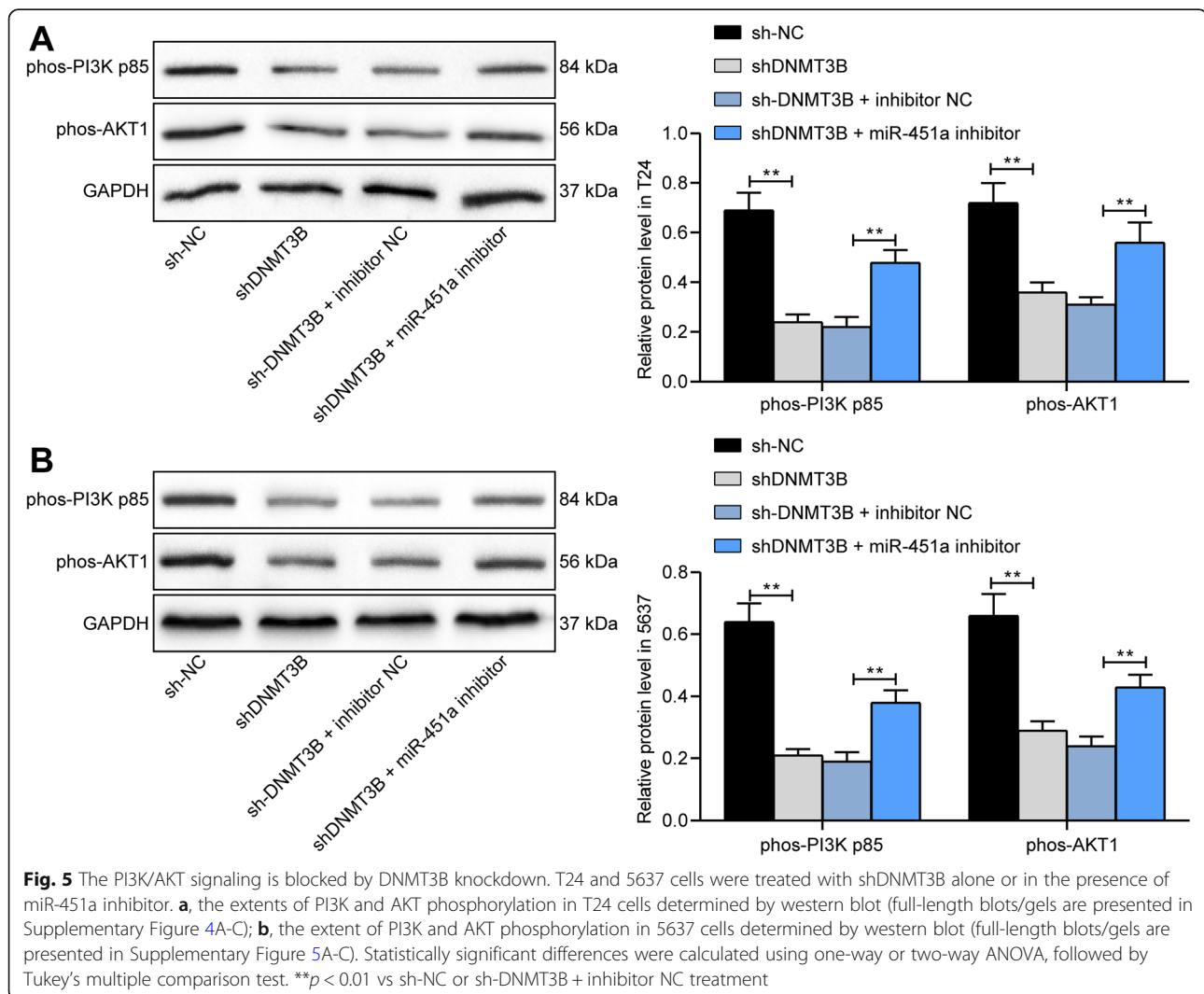
The PI3K/AKT signaling is disrupted by shDNMT3B

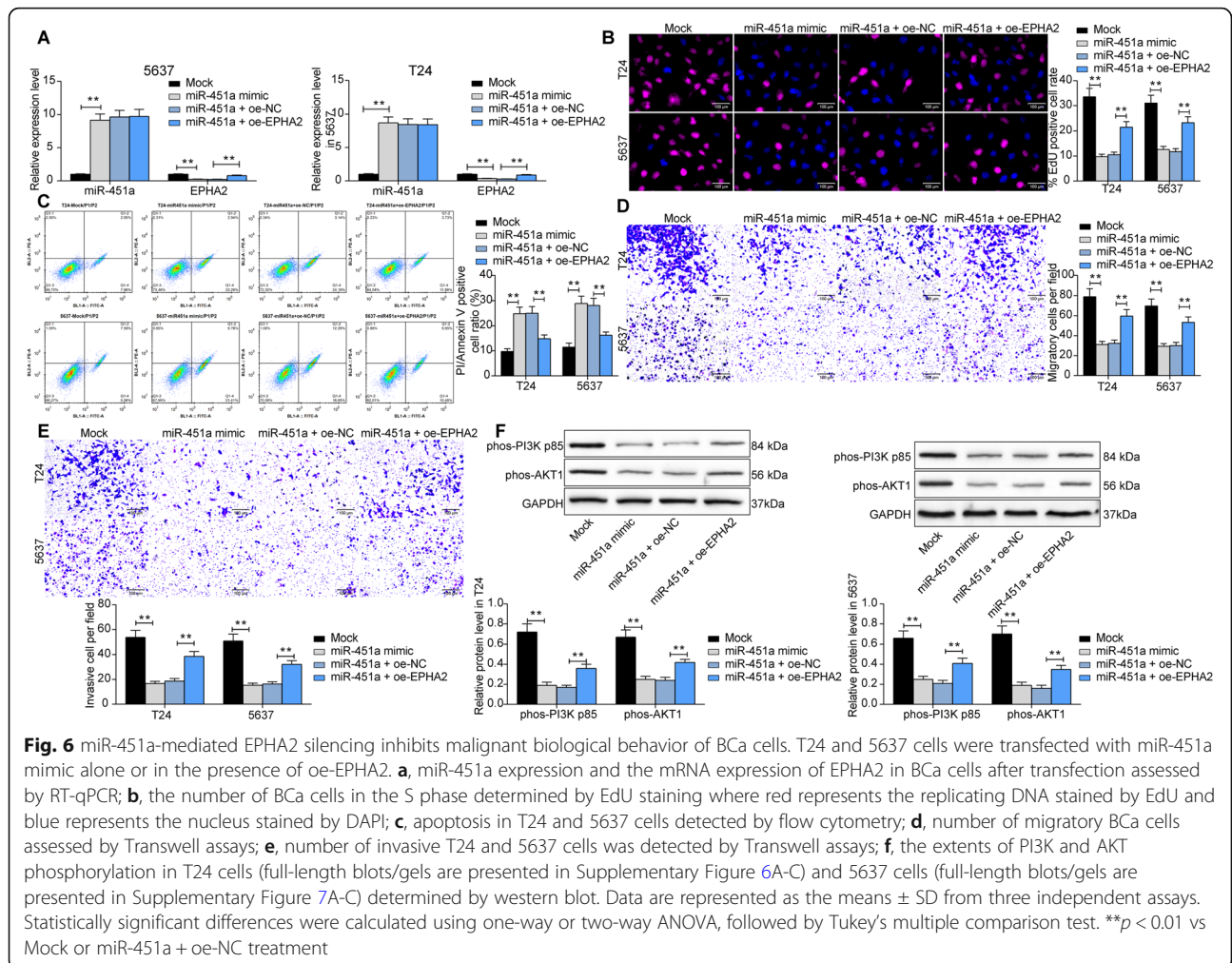
On the basis of our findings in Fig. 4, we observed that the PI3K/AKT signaling was significantly enriched, so we used western blot to assess the extent of PI3K p85 and AKT1 phosphorylation in T24 and 5637 cells. We found that their phosphorylation levels were significantly

inhibited in cells poorly-expressed DNMT3B. The extents of PI3K p85 and AKT1 phosphorylation were significantly restored (Fig. 5a, b) after further transfection using miR-451a inhibitor.

miR-451a-mediated EPHA2 silencing inhibits malignant biological behavior of BCa cells

To further validate the effect of the miR-451a/EPHA2 axis on BCa cell growth, we overexpressed miR-451a in T24 and 5637 cells, and further transfected EPHA2 overexpression plasmids in cells. We validated the transfection was successful (Fig. 6a) by RT-qPCR. miR-451a mimic notably inhibited the proliferative activity of T24 and 5637 cells; however, further increasing the expression of EPHA2 in the cells remarkably weakened the inhibition of miR-451a mimic on cell activity (Fig. 6b). Moreover, we further analyzed T24 and 5637 cell apoptosis by flow cytometry after PI/Annexin V staining. Overexpression of miR-451a significantly promoted cell





apoptosis, but oe-EPHA2 significantly inhibited miR-451a mimic-induced apoptosis (Fig. 6c). Subsequently, we used Transwell assays to verify the migration and invasion capacities of T24 and 5637 cells. The cell migration and invasion were significantly hampered after overexpression of miR-451a, which was mitigated by oe-EPHA2 (Fig. 6d, e). Lastly, the extent of PI3K/AKT phosphorylation in T24 and 5637 cells was assessed. Similarly, the blockage of miR-451a mimic on the PI3K/AKT signaling was antagonized by oe-EPHA2 (Fig. 6f).

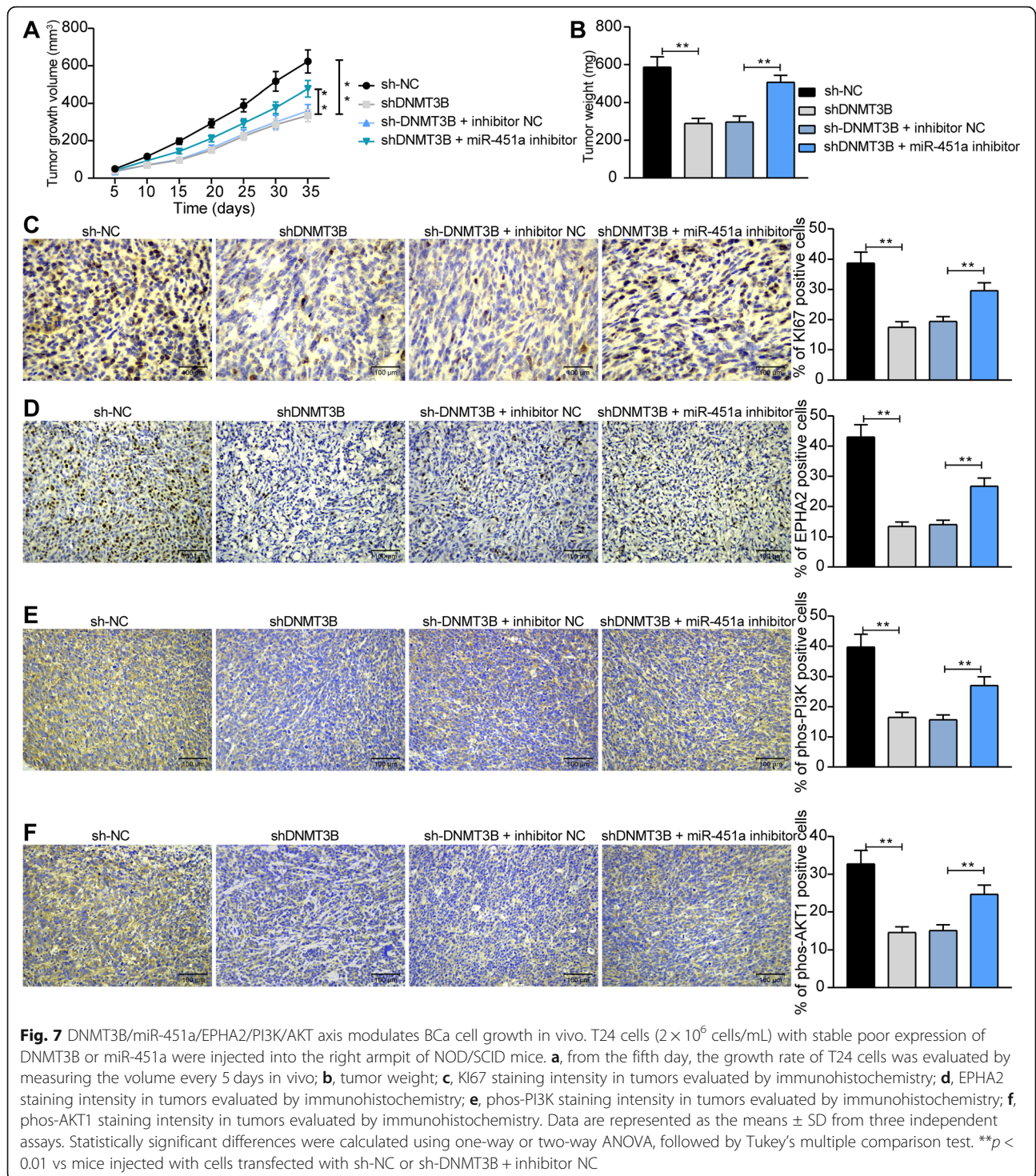
The DNMT3B/miR-451a/EPHA2/PI3K/AKT axis involves in the progression of BCa in vivo

To assess the effect of the DNMT3B/miR-451a axis on the development of BCa, we injected T24 cells (2×10^6 cells/mL) stably poor-expressing DNMT3B or miR-451a into the right armpit of NOD/SCID mice. Tumor volume was measured every 5 days from the fifth day after injection to assess the growth rate of T24 cells in vivo. The growth rate of T24 cells with poor expression of DNMT3B was significantly decreased, but under the

further action of miR-451a inhibitor, the growth rate of T24 cells in vivo was significantly increased (Fig. 7a). On the 35th day after injection, the weight of tumors formed by T24 cells in NOD/SCID mice showed the same experimental trend (Fig. 7b) as the volume. We then used immunohistochemistry to detect the staining intensity of KI67, EPHA2, phos-PI3K and phos-AKT1 in tumors. The staining intensity of KI67, EPHA2, phos-PI3K and phos-AKT1 in tumors decreased significantly after DNMT3B silencing. While in the presence of miR-451a inhibitor, the staining intensity of KI67, EPHA2, phos-PI3K and phos-AKT1 was notably restored (Fig. 7c-f).

Discussion

BCa is the 7th most prevalent cancer in male and the 17th most prevalent in female in a global range [16]. The miRNA signatures in BCa have been characterized, but the exact role of miRNA in the pathogenesis of BCa remains much less explored. In this study, the expression of miR-451a was significantly lower in serum of BCa patients than in normal controls, which was tightly



linked to the hypermethylation of its promoter region. In addition, miR-451a promoter region was methylated by DNMT3B. Moreover, loss- and gain-of-function analyses manifested that DNMT3B knockdown curtailed the proliferation, migration, and invasion of BCa cells, while induced apoptosis, which were reversed by miR-451a inhibitor. Further investigation disclosed that the

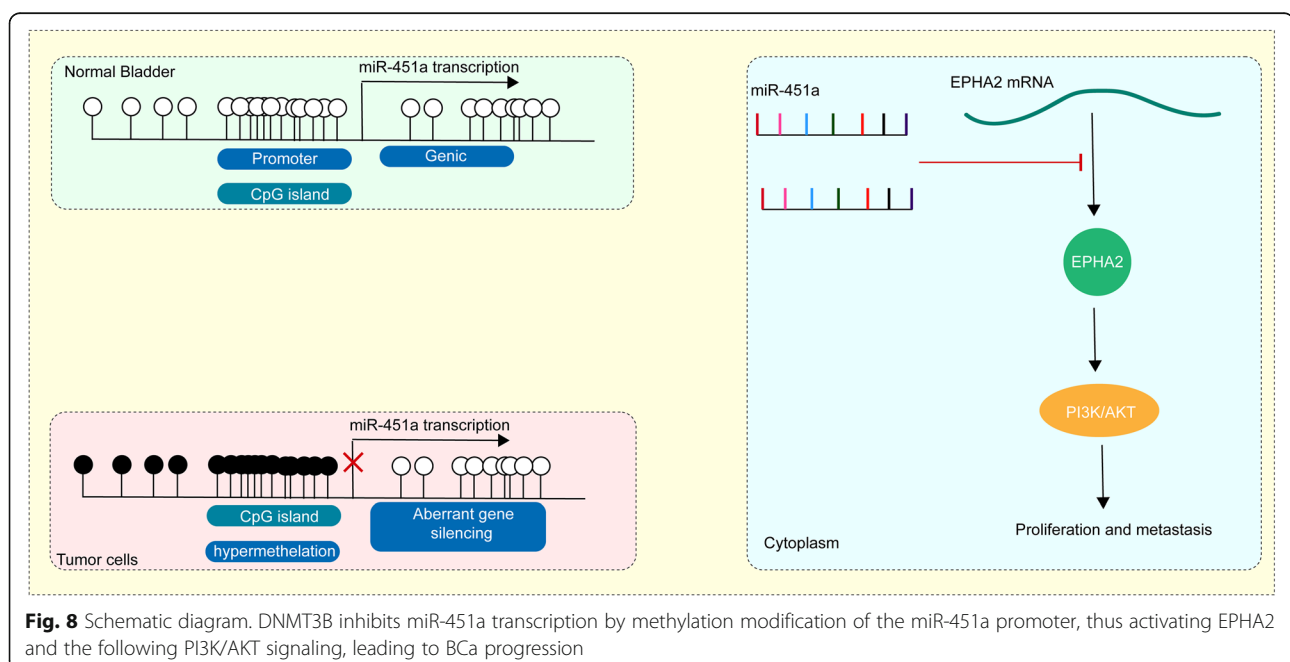
EPHA2/PI3K/AKT axis was participated in the BCa cell growth mediated by DNMT3B and miR-451a. These findings have highlighted the carcinostatic role of miR-451a in BCa.

The carcinostatic role of miR-451a has been substantiated in papillary thyroid carcinoma [17], lung cancer [18] as well as prostate cancer [19]. Likewise, our

bioinformatics tools revealed that BCa patients with higher miR-451a expression benefitted from longer survival, hinting the possible prognostic role of miR-451a in BCa. In addition, we confirmed that the dysregulation of miR-451a in BCa was associated with hypermethylation of its promoter region. In hepatocellular carcinoma cells, the CpG islands surrounding miR-433 were methylated, and the DNA methylation agent 5-aza-dC notably stimulated the expression of miR-433 [20]. Consistently, 5-aza-dC also induced miR-451a expression in BCa cells in the current study, further confirming the association between miR-451a downregulation and hypermethylation in BCa cells. miR-29b-3p has been validated to regulate the progression of BCa via targeting DNMT3B [21]. Conversely, the expression of some miRNAs can be modulated by DNA methylation, which indicated the linkages between miRNAs and epigenetic mechanisms [22]. For instance, Flap endonuclease 1 was proved to interact with DNMT3A to repress miR-200a-5p expression mediated by methylation in breast cancer [12]. In line with those previous evidence, our assays validated that knockdown of DNMT3B reduced miR-451a methylation, while enhanced miR-451a expression in BCa. In addition, rescue experiments suggested that the inhibitory role of DNMT3B knockdown on BCa cell proliferation, migration and invasion was abrogated by miR-451a inhibitor, further evidencing the interaction between DNMT3B and miR-451a as well as their roles in BCa.

Subsequently, our KEGG enrichment suggested that the PI3K/AKT signaling was recruited in BCa. In fact, 40% of BCa patients demonstrated the PI3K/AKT signaling overactivation [23]. In addition, targeting this

signaling has been reported as a possible therapeutic target in BCa [24, 25]. Our observations displayed that DNMT3B knockdown disrupted the PI3K/AKT signaling in BCa cells, which was reversed by miR-451a inhibitor. Multi-omics analysis and spontaneous metastatic mouse models performed by So et al. also documented that DNMT3B altered multiple pathways including PI3K/AKT [26]. While miR-451a played a tumor suppressive role in gastric cancer via mediation of the PI3K/AKT signaling [13]. Furthermore, EPHA2 was identified to be an upstream gene of the PI3K/AKT signaling by our KEGG analysis. EPHA2 was found to be required for progranulin-induced biological activity and cisplatin chemosensitivity in BCa [15]. Besides, EPHA2 was involved in the inhibition of angiogenesis mediated by leflunomide in BCa [27]. Promoted EPHA2 expression in cancer cells is linked to a dismal prognosis because of recurrence as a consequence of enhanced metastasis [28]. As for its upstream miRNAs, EPHA2 has been indicated to be targeted by different miRNAs to participate the development of various cancers, including non-small cell lung cancer [29], hepatocellular carcinoma [30] as well as colorectal cancer [31]. After the validation of the targeting relationship between EPHA2 and miR-451a in BCa cells, we carried out rescue experiments again. A series of assays validated that overexpression of EPHA2 rescued the tumor suppressive role of miR-451a in BCa cells. Our in vitro findings were reproduced on nude mice where shDNMT3B slowed down tumor growth, while miR-451a inhibitor partially restored the tumorigenicity of T24 cells with the involvement of EPHA2/PI3K/AKT axis.



Conclusion

Our study demonstrated that miR-451a was reduced in BCa cells. Poor expression of miR-451a was associated with its promoter methylation induced by DNMT3B. In addition, we proposed that miR-451a played an essential role in the proliferation, migration, and invasion of BCa cells by binding to EPHA2 and impairing the PI3K/AKT signaling (Fig. 8). Therefore, miR-451a may act as a prognostic marker for BCa patients and a potential target for the treatment of BCa.

Supplementary information

Supplementary information accompanies this paper at <https://doi.org/10.1186/s12885-020-07523-8>.

Additional file 1.

Abbreviations

ANOVA: Analysis of variance; BCa: Bladder cancer; BLCA: Bladder urothelial carcinoma; ChIP: Chromatin immunoprecipitation; DNMT3B: DNA methyltransferase 3B; EPHA2: Erythropoietin-producing hepatocellular receptor tyrosine kinase class A2; FBS: Fetal bovine serum; GAPDH: Glyceraldehyde-3-phosphate dehydrogenase; GEO: Gene Expression Omnibus; HRP: Horseradish peroxidase; KEGG: Kyoto Encyclopedia of Genes and Genomes; MSP: Methylation-specific PCR; PI: Propidium iodide; TUNEL: Terminal deoxynucleotidyl transferase (TdT)-mediated dUTPbiotin nick end labeling; DMEM: Dulbecco's modified Eagle's medium

Acknowledgements

Not applicable.

Authors' contributions

BBL and WS conceived and designed the studies. BBL, WYG, LQL and ZXC performed experiments. XHY, JML and YYG analyzed the data. BBL and WS drafted the manuscript. All authors read and approved the final manuscript.

Funding

This work was supported by Natural Science Research Projects of Universities of Anhui Province (KJ2019A0308), National Natural Science Foundation of China (81702495) and Anhui Natural Science Foundation (1808085QH279). The funding bodies had no role in the design of the study and collection, analysis, and interpretation of data and in writing the manuscript.

Availability of data and materials

All the data generated or analyzed during this study are included in this published article.

Ethics approval and consent to participate

All animal experiments were compliant with ethic regulations and approved by Institutional Animal Care & Use Committee of the First Affiliated Hospital of Bengbu Medical College.

Consent for publication

Not applicable.

Competing interests

All authors declare that there is no conflict of interests in this study.

Received: 30 July 2020 Accepted: 14 October 2020

Published online: 21 October 2020

References

- Siegel RL, Miller KD, Jemal A. Cancer statistics, 2020. *CA Cancer J Clin*. 2020; 70(1):7–30.
- Boormans JL, Zwarthoff EC. Limited funds for bladder Cancer research and what can we do about it. *Bladder Cancer*. 2016;2(1):49–51.
- Kamat AM, Hahn NM, Efsthathiou JA, Lerner SP, Malmstrom PU, Choi W, et al. Bladder cancer. *Lancet*. 2016;388(10061):2796–810.
- Bartel DP. MicroRNAs: target recognition and regulatory functions. *Cell*. 2009;136(2):215–33.
- Braicu C, Cojocneanu-Petric R, Chira S, Truta A, Floares A, Petrut B, et al. Clinical and pathological implications of miRNA in bladder cancer. *Int J Nanomedicine*. 2015;10:791–800.
- Matsushita R, Seki N, Chiyomaru T, Inoguchi S, Ishihara T, Goto Y, et al. Tumour-suppressive microRNA-144-5p directly targets CCNE1/2 as potential prognostic markers in bladder cancer. *Br J Cancer*. 2015;113(2):282–9.
- Shimizu T, Suzuki H, Nojima M, Kitamura H, Yamamoto E, Maruyama R, et al. Methylation of a panel of microRNA genes is a novel biomarker for detection of bladder cancer. *Eur Urol*. 2013;63(6):1091–100.
- Chang C, Liu J, He W, Qu M, Huang X, Deng Y, et al. A regulatory circuit HP1gamma/miR-451a/c-Myc promotes prostate cancer progression. *Oncogene*. 2018;37(4):415–26.
- Ying Y, Li J, Xie H, Yan H, Jin K, He L, et al. CCND1, NOP14 and DNMT3B are involved in miR-502-5p-mediated inhibition of cell migration and proliferation in bladder cancer. *Cell Prolif*. 2020;53(2):e12751.
- Zo RB, Long Z. MiR-124-3p suppresses bladder cancer by targeting DNA methyltransferase 3B. *J Cell Physiol*. 2018;234(1):464–74.
- Xu X, Zhu Y, Liang Z, Li S, Xu X, Wang X, et al. c-Met and CREB1 are involved in miR-433-mediated inhibition of the epithelial-mesenchymal transition in bladder cancer by regulating Akt/GSK-3beta/Snail signaling. *Cell Death Dis*. 2016;7:e2088.
- Zeng X, Qu X, Zhao C, Xu L, Hou K, Liu Y, et al. FEN1 mediates miR-200a methylation and promotes breast cancer cell growth via MET and EGFR signaling. *FASEB J*. 2019;33(10):10717–30.
- Mao S, Wu Y, Wang R, Guo Y, Bi D, Ma W, et al. Overexpression of GAS6 promotes cell proliferation and invasion in bladder Cancer by activation of the PI3K/AKT pathway. *Onco Targets Ther*. 2020;13:4813–24.
- Yao J, Qian K, Chen C, Liu X, Yu D, Yan X, et al. ZNF139/circZNF139 promotes cell proliferation, migration and invasion via activation of PI3K/AKT pathway in bladder cancer. *Aging (Albany NY)*. 2020;12(10):9915–34.
- Buraschi S, Neill T, Xu SQ, Palladino C, Belfiore A, Iozzo RV, et al. Progranulin/EphA2 axis: a novel oncogenic mechanism in bladder cancer. *Matrix Biol*. 2020;S0945-053X(20)30038-X. <https://doi.org/10.1016/j.matbio.2020.03.009>. Epub ahead of print. PMID: 32417448.
- Burger M, Catto JW, Dalbagni G, Grossman HB, Herr H, Karakiewicz P, et al. Epidemiology and risk factors of urothelial bladder cancer. *Eur Urol*. 2013; 63(2):234–41.
- Wang Q, Shang J, Zhang Y, Zhou Y, Tang L. MiR-451a restrains the growth and metastatic phenotypes of papillary thyroid carcinoma cells via inhibiting ZEB1. *Biomed Pharmacother*. 2020;127:109901.
- Tao L, Shu-Ling W, Jing-Bo H, Ying Z, Rong H, Xiang-Qun L, et al. MiR-451a attenuates doxorubicin resistance in lung cancer via suppressing epithelial-mesenchymal transition (EMT) through targeting c-Myc. *Biomed Pharmacother*. 2020;125:109962.
- Liu Y, Yang HZ, Jiang YJ, Xu LQ. miR-451a is downregulated and targets PSM88 in prostate cancer. *Kaohsiung J Med Sci*. 2020;36(7):494–500.
- Yang Z, Tsuchiya H, Zhang Y, Hartnett ME, Wang L. MicroRNA-433 inhibits liver cancer cell migration by repressing the protein expression and function of cAMP response element-binding protein. *J Biol Chem*. 2013; 288(40):28893–9.
- Lv M, Zhong Z, Huang M, Tian Q, Jiang R, Chen J. lncRNA H19 regulates epithelial-mesenchymal transition and metastasis of bladder cancer by miR-29b-3p as competing endogenous RNA. *Biochim Biophys Acta Mol Cell Res*. 2017;1864(10):1887–99.
- Wu P, Cao Z, Wu S. New Progress of epigenetic biomarkers in urological Cancer. *Dis Markers*. 2016;2016:9864047.
- Hindy JR, Souaid T, Kourie HR, Kattan J. Targeted therapies in urothelial bladder cancer: a disappointing past preceding a bright future? *Future Oncol*. 2019;15(13):1505–24.
- Ching CB, Hansel DE. Expanding therapeutic targets in bladder cancer: the PI3K/Akt/mTOR pathway. *Lab Invest*. 2010;90(10):1406–14.
- Houede N, Pourquier P. Targeting the genetic alterations of the PI3K-AKT-mTOR pathway: its potential use in the treatment of bladder cancers. *Pharmacol Ther*. 2015;145:1–18.
- So JY, Skrypek N, Yang HH, Merchant AS, Nelson GW, Chen WD, et al. Induction of DNMT3B by PGE2 and IL6 at distant metastatic sites promotes

- epigenetic modification and breast Cancer colonization. *Cancer Res.* 2020; 80(12):2612–27.
27. Chu M, Zhang C. Inhibition of angiogenesis by leflunomide via targeting the soluble ephrin-A1/EphA2 system in bladder cancer. *Sci Rep.* 2018;8(1):1539.
 28. Tandon M, Vemula SV, Mittal SK. Emerging strategies for EphA2 receptor targeting for cancer therapeutics. *Expert Opin Ther Targets.* 2011;15(1):31–51.
 29. Yu L, Chen D, Song J. LncRNA SNHG16 promotes non-small cell lung cancer development through regulating EphA2 expression by sponging miR-520a-3p. *Thorac Cancer.* 2020;11(3):603–11.
 30. Tian JH, Liu WD, Zhang ZY, Tang LH, Li D, Tian ZJ, et al. Influence of miR-520e-mediated MAPK signalling pathway on HBV replication and regulation of hepatocellular carcinoma cells via targeting EphA2. *J Viral Hepat.* 2019; 26(4):496–505.
 31. De Robertis M, Mazza T, Fusilli C, Loiacono L, Poeta ML, Sanchez M, et al. EphB2 stem-related and EphA2 progression-related miRNA-based networks in progressive stages of CRC evolution: clinical significance and potential miRNA drivers. *Mol Cancer.* 2018;17(1):169.

Publisher's Note

Springer Nature remains neutral with regard to jurisdictional claims in published maps and institutional affiliations.

Ready to submit your research? Choose BMC and benefit from:

- fast, convenient online submission
- thorough peer review by experienced researchers in your field
- rapid publication on acceptance
- support for research data, including large and complex data types
- gold Open Access which fosters wider collaboration and increased citations
- maximum visibility for your research: over 100M website views per year

At BMC, research is always in progress.

Learn more biomedcentral.com/submissions

